

# Self-assembled monolayers of gold nanostars: a convenient tool for near-IR photothermal biofilm eradication†

Cite this: *Chem. Commun.*, 2014, 50, 1969Received 13th November 2013,  
Accepted 16th December 2013

DOI: 10.1039/c3cc48667b

www.rsc.org/chemcomm

Piersandro Pallavicini,<sup>\*a</sup> Alice Donà,<sup>a</sup> Angelo Taglietti,<sup>a</sup> Paolo Minzioni,<sup>b</sup> Maddalena Patrini,<sup>c</sup> Giacomo Dacarro,<sup>c</sup> Giuseppe Chirico,<sup>d</sup> Laura Sironi,<sup>d</sup> Nora Bloise,<sup>e</sup> Livia Visai<sup>e,g</sup> and Leonardo Scarabelli<sup>f</sup>

**Monolayers of gold nanostars (GNS) are grafted on mercaptopropyl-trimethoxysilane-coated glass slides. In the formed monolayers the localized surface plasmon resonance of GNS can be tuned in the 700–1100 nm range. Upon laser excitation of the nearIR LSPR an efficient photothermal response is observed, inducing local hyperthermia and efficient killing of *Staphylococcus aureus* biofilms.**

Biofilms are sessile microbial communities, usually constituted by the Gram+ *Staphylococcus aureus* and *Staphylococcus epidermidis*, embedded in a self-produced extracellular polymer matrix. They may develop on the surface of prostheses, catheters and implants, leading to severe infections in an impressive number of hospitalized patients.<sup>1</sup> Conventional antibiotics do not eradicate biofilms from the surfaces where they have formed and often surgical removal of the implant is the only affordable solution. It has been proposed that coating medical devices with Ag nanoparticles prevents biofilm formation but with controversial results,<sup>2a,b</sup> as Ag nanoparticles are effective towards Gram– bacterial strains but much less towards Gram+.<sup>2c,d</sup> We propose here a new approach based on gold nanostars (GNS). Gold is not intrinsically antibacterial but GNS possess two or more localized surface plasmon resonances (LSPR) that

undergo thermal relaxation upon irradiation. Moreover, at least one LSPR falls in the near-IR range (NIR, 750–1100 nm)<sup>3</sup> where tissues and blood are semi-transparent. Following some examples of glass surfaces coated with gold nanoparticle monolayers,<sup>4</sup> we have now prepared bulk glass materials coated with a GNS monolayer, that proved to be very efficient in photothermal biofilm laser-treatment against *S. aureus* biofilms, suggesting the possibility of fabricating medical devices with the same coating: once internalized, they would not need to be removed if a biofilm is formed on their surface but may be treated *in situ*, *i.e.* through tissues.

GNS are prepared in water according to a seed-growth method developed by us using laurylsulfobetaine (LSB) as the directing and coating agent.<sup>5a</sup> The obtained colloidal solutions are mixtures containing mainly asymmetric branched gold nanoparticles (70–80%) and a lower percentage of symmetric 6-branched nanostars, see Fig. 1B for a

<sup>a</sup> inLAB, Department of Chemistry, University of Pavia, v.le Taramelli 12, 27100 Pavia, Italy. E-mail: piersandro.pallavicini@unipv.it; Fax: +39 382528544; Tel: +39 382987336

<sup>b</sup> Department of Electrical, Computer, and Biomedical Engineering, and CNISM, University of Pavia, v. A. Ferrata, 5A, 27100 Pavia, Italy

<sup>c</sup> Department of Physics, University of Pavia, v. Bassi, 6, 27100 Pavia, Italy

<sup>d</sup> Department of Physics “G. Occhialini”, University of Milano Bicocca, Piazza della Scienza 3, 20126 Milano, Italy

<sup>e</sup> Department of Molecular Medicine, Center for Tissue Engineering (C.I.T.), INSTM UDR of Pavia, University of Pavia, 27100 Pavia, Italy

<sup>f</sup> CIC biomAGUNE, Center for Cooperative Research in Biomaterials, Paseo de Miramón 182, 20009 Donostia-San Sebastián, Spain

<sup>g</sup> Department of Occupational Medicine, Ergonomy and Disability, Lab.

Nanotechnology, Salvatore Maugeri Foundation, IRCCS, 27100 Pavia, Italy

† Electronic supplementary information (ESI) available: Detailed experimental procedures; list of reactants and materials; slide photographs; SEM images; normalized UV/Vis spectra and Au  $\mu\text{g cm}^{-2}$  calibration curve; UV-Vis-NIR spectra of round slides used for biofilms. See DOI: 10.1039/c3cc48667b

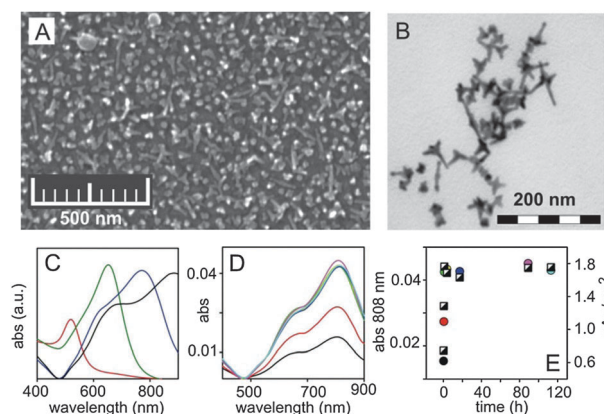


**Fig. 1** (A) SEM image of a glass|MPTS|GNS slide. (B) TEM image of GNS from the colloidal solution used to prepare the slide imaged in (A). (C) Representative absorption spectra recorded on glass slides prepared from colloidal solutions of GNS with different LSPR positions. (D) Absorption spectra (normalised at 480 nm) obtained for glass|MPTS slides dipped for different times in a GNS solution. (E) Colored circles are the normalized absorbance values at 808 nm (left vertical axis) from panel (D), as a function of time; colors correspond between (E) and (D). Half-filled squares are the Au  $\mu\text{g cm}^{-2}$  values obtained by ICP-OES for the same slides (right vertical axis).

representative TEM image. Their absorption spectrum in solution is dominated by the LSPR of the main component, whose maximum can be positioned in the 750–1150 nm range as a function of the reaction conditions. Adhesion of a monolayer of GNS on glass is obtained by formation of first a monolayer of MPTS on the surface, according to an established procedure.<sup>6</sup> The obtained glass|MPTS surfaces are then dipped into a colloidal solution of GNS ( $\text{Au} = 0.06\text{--}0.07 \text{ g L}^{-1}$ ), typically for 18 hours, yielding glass|MPTS|GNS surfaces, with the formation of thiolate–gold bonds (all experimental details in ESI,† Sections S1 and S2).

The weak nature of the LSB–Au interaction<sup>5b</sup> favours the facile LSB surface displacement by the MPTS thiol groups and efficient GNS adhesion. The slides are sonicated in water 3 times for 3 min before use and dried with a  $\text{N}_2$  flux. They can be kept in air at room temperature, under light exposure, with no degradation after 3 months (as checked with UV-Vis spectra). Control experiments on plain glass gave no coating. GNS-bearing slides are intensely colored but transparent (photographs in ESI,† Fig. S3A–E) and absorption spectra are directly recorded on dry slides using a common UV-Vis spectrophotometer. The position of the LSPR maximum can be placed at the desired wavelength with a large interval (550–1100 nm), see *e.g.* Fig. 1C, depending on the LSPR of the chosen coating solution. The surface is densely populated by GNS, as shown by Scanning Electron Microscope (SEM) images, Fig. 1A (ESI,† Fig. S4A and B for larger images). The grafted GNS maintain the shape they have in the coating colloidal solution. A LSPR blue shift of 52 nm (average on 70 preparations,  $\sigma = 10 \text{ nm}$ ) is observed on passing from the colloidal solution in water to the monolayer on glass in air (ESI,† Fig. S3F), due to change in the local refractive index ( $n$ ). Glass|MPTS|GNS surfaces prepared on the internal wall of an optical glass cuvette, then filled with different solvents (ESI,† Fig. S5), show a linear trend for  $\lambda_{\text{max}}$  vs.  $n$  with a  $300 \text{ nm}/n$  unit variation, and when water is the solvent  $\lambda_{\text{max}}$  reaches a similar value as in colloidal solution. Glass|MPTS|GNS slides prepared with dipping times shorter than 18 hours show a less dense coating than seen in Fig. 1A, which corresponds to a less intense UV-Vis-NIR absorption (ESI,† Fig. S4C for SEM images). This prompted us to study the kinetics of coating. Using colloidal solutions with  $\lambda_{\text{max}} = 850 \text{ nm}$  ( $\lambda_{\text{max}}$  on glass =  $808 \text{ nm}$ ), glass|MPTS slides are taken off at different times along a period of 140 hours. Absorption spectra are recorded on each slide and the total Au content determined by fully oxidizing the GNS monolayer in a small measured volume of aqua regia (3.0 mL). This is finally analysed using standard techniques for diluted cations in solution (ICP-OES, inductively coupled plasma optical emission spectroscopy). Spectra are normalized by setting the absorbance to zero at 480 nm (Fig. 1D) and a sharp ascending/plateau trend is obtained by plotting Abs at  $\lambda_{\text{max}}$  vs. time (Fig. 1E, coloured circles). The trend parallels the quantity of Au per  $\text{cm}^2$  found by oxidation/ICP-OES, Fig. 1E (half-filled squares). Full coating is reached in <18 hours, confirming that the routine time for preparation is suitable. Many slides were prepared with 18 hours coating time in GNS solutions from different syntheses, and the total Au per  $\text{cm}^2$  calculated, with variations from preparation to preparation, albeit in a limited range ( $1.5\text{--}3.5 \mu\text{g cm}^{-2}$ ). By normalizing the absorption spectra at 480 nm and determination

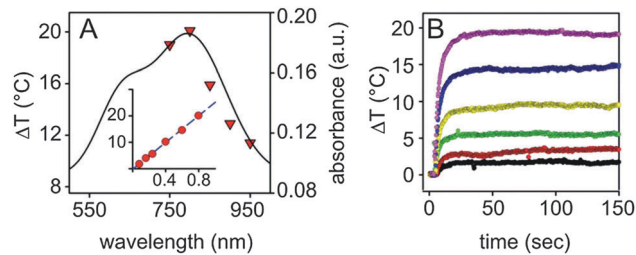


Fig. 2 (A) Black line: absorption spectrum of the slide for laser irradiation. Red triangles are  $\Delta T$  values (left vertical axis) found using the same irradiance ( $0.8 \text{ W cm}^{-2}$ ) with laser sources of different wavelengths. Inset:  $\Delta T$  vs. irradiance at 800 nm. (B)  $\Delta T$  vs. time, laser at 800 nm, irradiance 0.08 (black), 0.16 (red), 0.24 (green), 0.40 (yellow), 0.60 (blue) and  $0.8 \text{ W cm}^{-2}$  (pink).

of the total gold quantity on the slide by ICP-OES, a linear plot for Abs at LSPR maximum vs. Au per  $\text{cm}^2$  is obtained (ESI,† Fig. S6A). We used this as a calibration plot in all further preparations, in order to quickly calculate the Au per  $\text{cm}^2$  surface concentration on each freshly prepared slide. For the sake of uniformity, in all the following experiments slides were used with Au content only in the  $2.0\text{--}3.0 \mu\text{g cm}^{-2}$  range. The efficient photothermal properties of the GNS used in this work have been already demonstrated in their colloidal solutions.<sup>7</sup> Now we use dry glass|MPTS|GNS slides with LSPR maximum at  $\sim 800 \text{ nm}$  (Fig. 2A). The slides were irradiated with continuous laser sources at 750, 800, 850, 900 and 950 nm, with irradiance of  $0.80 \text{ W cm}^{-2}$ . The  $T$  increase is measured as a function of time using a thermocamera (see ESI,† S1).

The highest  $\Delta T$  is found when using a laser source with a wavelength exactly matching the  $\lambda_{\text{max}}$  of LSPR (800 nm), while the  $\Delta T$  trend smoothly follows the LSPR band profile (red triangles, Fig. 2A). When using the 800 nm source, the power was also varied, showing that  $\Delta T$  linearly increases from 2 to  $20 \text{ }^\circ\text{C}$  when irradiance increases from  $0.08$  to  $0.8 \text{ W cm}^{-2}$  (Fig. 2A, inset). Fig. 2B shows the  $\Delta T$  vs. time trends at each irradiance (laser at 800 nm), showing steep ascending-plateau profiles with a rapidly reached maximum equilibrium temperature (<20 s). It is worth mentioning that a significant increase in  $T$  is observed using a laser beam intensity ( $0.08 \text{ W cm}^{-2}$ ) four times lower than the maximum permitted exposure for skin, as established by the American National Standards Institute (ANSI) Laser Safety Standards.<sup>3c,d,8</sup>

For the antibiofilm studies a series of 32 round glass slides (diameter 1.0 cm) were prepared, with LSPR centred at  $802 (\sigma = 12) \text{ nm}$  (ESI,† Fig. S7) and a gold surface concentration of  $3.0 (\sigma = 0.4) \mu\text{g cm}^{-2}$ . The microorganism used is a methicillin-resistant *S. aureus* LP strain, which was shown to be an efficient biofilm producer.<sup>1c</sup> For biofilm growth an overnight culture of *S. aureus* LP was diluted at 1:50 in tryptone soy broth (TSB) containing 0.25% glucose, and aliquots (0.500 mL) of the diluted bacterial suspension were inoculated into 24-well microplates containing either plain glass slides or glass|MPTS|GNS slides, and incubated for 16 hours at  $37 \text{ }^\circ\text{C}$ . Some of the wells were laser-treated with a AlGaAs laser diode with emitting light at 808 nm, irradiance of  $0.090 \text{ W cm}^{-2}$  (also taking into account the  $\approx 24\%$  loss introduced by the plate bottom), and a waist with a diameter matching that of the glass slides (ESI,† details and experimental set up). The exposure time to laser was 5, 10 and 30 minutes.

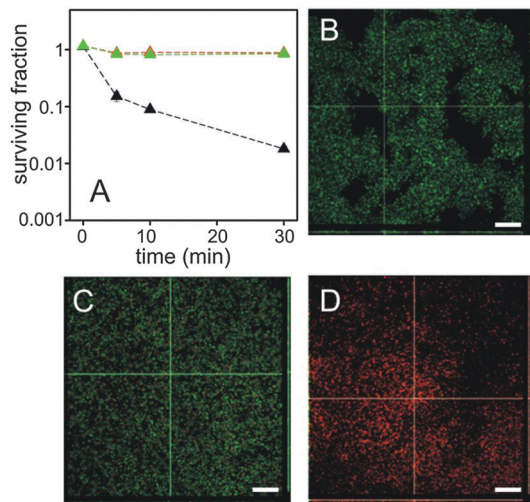


Fig. 3 (A) *S. aureus* viability vs. time (surviving fraction as CFU/CFU found on glass unexposed to laser); red triangles for plain glass irradiated with laser, green for glass|MPTS|GNS not irradiated, black for glass|MPTS|GNS irradiated with laser. The values are the means of the results from duplicate biofilms. Data are representative of three replicate experiments with similar results (see ESI† for error bars). (B–D) CLSM images of *S. aureus* biofilms grown on plain glass and irradiated with laser (B), on glass|MPTS|GNS unexposed (C), on glass|MPTS|GNS laser exposed (D); wavelength 808 nm, irradiance  $0.090 \text{ W cm}^{-2}$  for 30 min. Sagittal sections of the biofilms are shown below and to the right of each panel. Scale bar = 50  $\mu\text{m}$ .

Then, the biofilms were carefully scraped, sonicated, and then vortexed for 20 seconds to homogenize the samples. The samples were serially diluted, plated on the TSB agar plates, and incubated for 24 hours at  $37^\circ\text{C}$ . For each set of measurements, the control samples were biofilms grown on glass slides and unexposed to laser: the colony forming units (CFU) from bacteria grown on control samples are considered as 100%. Cell survival is expressed as the ratio of the CFU from bacteria grown on the other samples to that of the control. On biofilms grown on glass|MPTS|GNS slides a dramatic reduction of the CFU was observed with laser treatment (Fig. 3A, black triangles) with a decrease of one order of magnitude of the surviving fraction after 5 minutes irradiation and two orders of magnitude after 30 min. On the other hand, no reduction of the CFU was observed both on plain glass slides irradiated with laser (Fig. 3A, green triangles) and on glass|MPTS|GNS slides with no laser irradiation (Fig. 3A, red triangles). Biofilms were also studied by confocal laser scanning microscopy (CLSM), using a BacLight Live/Dead viability kit, according to an established procedure.<sup>9</sup> Biofilms grown overnight on plain glass and exposed for 30 min to laser (Fig. 3B) exhibited a green fluorescence (viable cells) and appeared organized as multilayered aggregates. A similar result was observed for the *S. aureus* biofilm grown on glass|MPTS|GNS slides but not irradiated with laser (Fig. 3C). Biofilms grown on glass|MPTS|GNS slides and irradiated at 808 nm for 30 min appeared uniformly red (dead cells) and more dispersed than the controls (Fig. 3D), see also ESI† Section S18 for images of enhanced graphical quality.

Photothermal therapy is a potentially powerful tool against biofilms.<sup>10</sup> In this communication we demonstrate that bulk glass surfaces bearing controlled microgram quantities of gold (up to  $3.0 \mu\text{g cm}^{-2}$ ) as firmly grafted, stable monolayers of nanostars can be prepared. Laser irradiation of the GNS monolayer at their NIR LSPR results in efficient photothermal conversion. Using irradiance values significantly lower than the maximum permissible exposure of skin, with a laser source at 808 nm we observed that the photothermal action of the GNS monolayer efficiently induces cell death in *S. aureus* biofilms by hyperthermia. This coating approach may be in principle also applied on steel, ITO, silica, *i.e.* any surface that is prone to MPTS functionalization. Using a laser source inside the biological “transparent” NIR window, our findings could lead to useful coatings for internalized medical devices and implants: biofilms that eventually form on their surface may be laser-treated *in situ*, avoiding surgical removal.

The authors thank Fondazione Cariplo (Project 2010-0454), Regione Lombardia (Project SAL-45), MIUR (PRIN 2010-2011 20109P1MH2\_003 and PRIN 2010-2011 NANOMED 2010FPTBSH\_009) for financial support, Dr Lucia Cucca for ICP-OES, M.S. Grandi and Laboratorio Arvedi of the University of Pavia for SEM inspection.

## Notes and references

- (a) J. W. Costerton, P. S. Stewart and E. P. Greenberg, *Science*, 1999, **284**, 1318–1322; (b) J. W. Costerton, R. Veeh, M. Shirliff, M. Pasmore, C. Post and G. Ehrlich, *J. Clin. Invest.*, 2003, **112**, 1466–1477; (c) M. Sharma, L. Visai, F. Bragheri, I. Cristiani, P. K. Gupta and P. Speziale, *Antimicrob. Agents Chemother.*, 2008, **52**, 299–305.
- (a) K. Vasilev, J. Cook and H. J. Griesser, *Expert Rev. Med. Devices*, 2009, **6**, 553–567; (b) S. Chernousova and M. Epple, *Angew. Chem., Int. Ed.*, 2013, **52**, 1636–1653; (c) A. Taglietti, Y. A. Diaz-Fernandez, E. Amato, L. Cucca, G. Dacarro, P. Grisoli, V. Necchi, P. Pallavicini, L. Pasotti and M. Patrini, *Langmuir*, 2012, **28**, 8140–8148; (d) G. Dacarro, L. Cucca, P. Grisoli, P. Pallavicini, M. Patrini and A. Taglietti, *Dalton Trans.*, 2012, **41**, 2456–2463.
- (a) J. Pérez-Juste, I. Pastoriza-Santos, L. M. Liz-Marzán and P. Mulvaney, *Coord. Chem. Rev.*, 2005, **249**, 1870–1901; (b) V. Guerrero-Martínez, S. Barbosa, I. Pastoriza-Santos and L. M. Liz-Marzán, *Curr. Opin. Colloid Interface Sci.*, 2011, **16**, 118–127; (c) H. Yuan, A. M. Fales and T. Vo-Dinh, *J. Am. Chem. Soc.*, 2012, **134**, 11358–11361; (d) H. Yuan, C. G. Khoury, C. M. Wilson, G. A. Grant, A. J. Bennett and T. Vo-Dinh, *Nanomedicine*, 2012, **8**, 1355–1366.
- (a) B. S. Flavel, M. R. Nussio, J. S. Quinton and J. G. Shapter, *J. Nanopart. Res.*, 2009, **11**, 2013–2022; (b) R. R. Bhat, D. A. Fischer and J. Genzer, *Langmuir*, 2002, **18**, 5640–5643.
- (a) A. Casu, E. Cabrini, A. Donà, A. Falqui, Y. A. Diaz-Fernandez, C. Milanese, A. Taglietti and P. Pallavicini, *Chem.-Eur. J.*, 2012, **18**, 9381–9390; (b) L. Sironi, S. Freddi, M. Caccia, P. Pozzi, L. Rossetti, P. Pallavicini, A. Donà, E. Cabrini, M. Gualtieri, I. Rivolta, A. Panariti, L. D’Alfonso, M. Collini and G. Chirico, *J. Phys. Chem. C*, 2012, **116**, 18407–18418.
- (a) P. Pallavicini, A. Taglietti, G. Dacarro, Y. A. Diaz-Fernandez, M. Galli, P. Grisoli, M. Patrini, G. Santucci De Magistris and R. Zanoni, *J. Colloid Interface Sci.*, 2010, **350**, 110–116; (b) Q. Su, X. Ma, J. Dong, C. Jiang and W. Qian, *ACS Appl. Mater. Interfaces*, 2011, **3**, 1873–1879.
- S. Freddi, L. Sironi, R. D’Antuono, D. Morone, A. Donà, E. Cabrini, L. D’Alfonso, M. Collini, P. Pallavicini, G. Baldi, D. Maggioni and G. Chirico, *Nano Lett.*, 2013, **13**, 2004–2010.
- ANSI, American National Standard for Safe Use of Lasers, Laser Institute of America, Orlando, FL, 2000.
- E. Saino, M. S. Sbarra, C. R. Arciola, M. Scavone, N. Bloise, P. Nikolov, F. Ricchelli and L. Visai, *Int. J. Artif. Organs*, 2010, **33**, 636–645.
- W. Jo and M. J. Kim, *Nanotechnology*, 2013, **24**, 195104–195111.